An ellipsoid-chain model for conjugated polymer solutions

Cheng K. Lee, Chi C. Hua, and Show A. Chen

Citation: J. Chem. Phys. **136**, 084901 (2012); doi: 10.1063/1.3687241
View online: http://dx.doi.org/10.1063/1.3687241
View Table of Contents: http://jcp.aip.org/resource/1/JCPSA6/v136/i8
Published by the American Institute of Physics.

An ellipsoid-chain model for conjugated polymer solutions

Cheng K. Lee,[1] Chi C. Hua,[2,a)] and Show A. Chen[3]
[1]*Research Center for Applied Sciences, Academia Sinica, Taipei 115, Taiwan*
[2]*Department of Chemical Engineering, National Chung Cheng University, Chia-Yi 621, Taiwan*
[3]*Department of Chemical Engineering, National Tsing Hua University, Hsin-Chu 30013, Taiwan*

(Received 2 August 2011; accepted 1 February 2012; published online 23 February 2012)

We propose an ellipsoid-chain model which may be routinely parameterized to capture large-scale properties of semiflexible, amphiphilic conjugated polymers in various solvent media. The model naturally utilizes the defect locations as pivotal centers connecting adjacent ellipsoids (each currently representing ten monomer units), and a variant umbrella-sampling scheme is employed to construct the potentials of mean force (PMF) for specific solvent media using atomistic dynamics data and simplex optimization. The performances, both efficacy and efficiency, of the model are thoroughly evaluated by comparing the simulation results on long, single-chain (i.e., 300-mer) structures with those from two existing, finer-grained models for a standard conjugated polymer (i.e., poly(2-methoxy-5-(2′-ethylhexyloxy)-1,4-phenylenevinylene) or MEH-PPV) in two distinct solvents (i.e., chloroform or toluene) as well as a hybrid, binary-solvent medium (i.e., chloroform/toluene = 1:1 in number density). The coarse-grained Monte Carlo (CGMC) simulation of the ellipsoid-chain model is shown to be the most efficient—about 300 times faster than the coarse-grained molecular dynamics (CGMD) simulation of the finest CG model that employs explicit solvents—in capturing elementary single-chain structures for both single-solvent media, and is a few times faster than the coarse-grained Langevin dynamics (CGLD) simulation of another implicit-solvent polymer model with a slightly greater coarse-graining level than in the CGMD simulation. For the binary-solvent system considered, however, both of the two implicit-solvent schemes (i.e., CGMC and CGLD) fail to capture the effects of conspicuous concentration fluctuations near the polymer-solvent interface, arising from a pronounced coupling between the solvent molecules and different parts of the polymer. Essential physical implications are elaborated on the success as well as the failure of the two implicit-solvent CG schemes under varying solvent conditions. Within the ellipsoid-chain model, the impact of synthesized defects on local segmental ordering as well as bulk chain conformation is also scrutinized, and essential consequences in practical applications discussed. In future perspectives, we remark on strategy that takes advantage of the coordination among various CG models and simulation schemes to warrant computational efficiency and accuracy, with the anticipated capability of simulating larger-scale, many-chain aggregate systems. © *2012 American Institute of Physics*. [http://dx.doi.org/10.1063/1.3687241]

I. INTRODUCTION

Computer simulations based on coarse-grained (CG) polymer models have recently received fast-growing attention for their ability to resolve molecular details—often inaccessible in experiment—that are essential to address many fundamental issues in polymer material sciences nowadays.[1–3] Compared with the traditional, atomistic molecular dynamics (AMD) schemes, the derivative CG schemes have opened new opportunities for assessing large-scale structural and dynamic (with proper time rescaling) properties that would otherwise pose significant challenges to contemporary computing resources. A renowned example is concerned with polymer solutions, where the focus is typically on the polymer chains and often the solvent molecules play only implicit roles. In this case, it is tempting to take a great step forward in coarse-graining the solvent particles while keeping their impact on the polymer molecule as intact as possible, especially for dilute solution where the essential interactions to capture are those between a polymer and the surrounding solvent molecules. The imperative issue of treating solvent molecules, explicitly or implicitly, in CG simulations has recently been extensively examined for conjugated polymer,[4–6] biopolymer,[7,8] and ionic solutions.[9] The general findings appear to encourage the use of more efficient, implicit-solvent models in capturing principal single-chain and/or aggregate structures, while there remain notable constraints under certain solution conditions that must be tackled, for instance, with the aid of a subsequent back-mapping to the atomistic level of model description—which nevertheless saves the overall computational time with near-equilibrium state so obtained. We mention, in particular, it has recently been demonstrated that a refined Langevin dynamics scheme, which utilized "measured" monomer diffusivities directly from an AMD simulation of the relevant solvent bath during the construction of fluctuation–dissipation forces acting on the polymer, may also satisfactorily

a)Author to whom correspondence should be addressed. Electronic mail: chmcch@ccu.edu.tw.

reproduce essential single-chain properties, both structural and dynamic, of a standard conjugated polymer under varying solvent conditions,[6] without invoking freely adjustable parameters on momoneric drag coefficient, as was often needed in a conventional Brownian dynamics scheme which subjects itself to no or little attribute of the specific solvent medium under consideration. Since only dilute, single-solvent media had been investigated, the general applicability of this (implicit-solvent) Langevin dynamics scheme is yet to be explored. In light of contemporary applications with conducting conjugated polymers, this major breakthrough allows computationally efficient forward/backward mappings to be carried out to reconcile capturing the equilibrium conformation of substantially long chains in solution and, later, localized structural features in the quenching state[5]—a traditionally challenging task for computer simulations that is nevertheless imperatively demanded by modern material sciences exploiting long-chain semiconductors in the fabrication of optoelectronic devices.

Developing efficient and reasonably accurate implicit-solvent CG models and simulation schemes is very important for polymer solution systems, especially when one is interested in large-scale supramolecular structures subject to varying medium properties, such as solvent type, polymer and salt concentrations.[7–9] Another way to promote computational efficiency is obviously to elevate the level of coarse-graining of the polymer molecule itself. For a semiflexible chain, like the cases with typical conjugated polymers and biopolymers, however, the prime challenge lies in the progressive inadequateness of conventional bead-spring picture underlying prevalent CG polymer models, because the chain takes rod-like or ellipsoidal shape for the segmental units mapped at increasingly enlarged CG level. For a similar reason, ellipsoid (or ellipsoid-chain) models had been exploited in a few pioneering researches on liquid crystalline polymers,[10,11] polycarbonate modifications,[12] and polymer melts.[13] In this study, we report the first model construction and performance evaluation of an ellipsoid-chain model, designed especially to capture single-chain and aggregation properties of typical conjugated polymers dissolved in various solvent media. The special feature lies in a substantially enlarged CG level as compared with existing (predictive) CG models, which typically considered monomer units or small molecular groups as the mapping length scale. This new CG polymer model, in fact, has morphed from a recent parameterization of conjugated oligomer within the classical Gay-Berne (GB) potential. We address in this paper how the central idea may be adopted to further incorporate chain connectivity, naturally, at defect locations connecting a string of ellipsoidal segments, as well as to suspend the segments in the desired solvent bath while establishing the potentials of mean force (PMF). In this way, the parameterized ellipsoid-chain model may promise to capture the effects of specific solvents (or solvent qualities) in a computationally much efficient manner.

As a systematic evaluation of the model's performance, the corresponding coarse-grained Monte Carlo (CGMC) simulation of the ellipsoid-chain model is scrutinized against the results for two existing, finer-grained polymer models in terms of both efficiency and efficacy, for two representative single-solvent media as well as a hybrid, binary-solvent system. Given that the proposed ellipsoid-chain model is also an ideal candidate for investigating the influence of synthesized defects, we later scrutinize the bulk and localized structural features of a conjugated polymer in solution, with varying degree of a ubiquitous synthesized defect—the tetrahedral defect. Based on the overall findings, we discuss the merits as well as major constraints of the three CG models under investigation, and remark on strategy that may be adopted to coordinate various CG models so as to tackle large-scale material properties in solution warranting both computational efficiency and accuracy.

This paper is organized as follows: Sec. II A provides some background of the polymer system under investigation, along with a briefing of two previously proposed CG models and attendant simulation schemes; Sec. II B offers more detailed descriptions of the construction and simulation scheme of a new ellipsoid-chain model aimed to capture large-scale material properties of specific conjugated polymer dissolved in various solvent media—so far only for dilute condition. Section III A evaluates the performances of all three CG models in predicting elementary single-chain structures in various single-solvent and binary-solvent media, while Sec. III B explores the impact of synthesized defect within the ellipsoid-chain model. Section IV remarks on future perspectives of coordinating existing CG models and schemes to meet the requirement of contemporary applications with conducting conjugated polymers, followed by concluding remarks in Sec. V.

II. SIMULATION PROTOCOL

A. Background

The central idea motivating multiscale coarse-grained simulations for polymer materials has been the quest to search for the largest molecular units that suffice capturing the physical properties of interest, while these "building units" may be pertinently coarse-grained into simple particles or segments of which the governing force laws are readily established from the simulations of finer-grained models,[1–3,7–9,12–17] usually beginning with AMD simulations of the atomistic polymer model. For the polymer species investigated, Fig. 1 depicts the physical pictures of a hierarchy of coarse-graining steps leading to polymer models that may be simulated increasingly more efficiently, and thus allow for accessibility of larger time/length scales. The delicate part, however, is that there remain no universal tactics guiding the exact pathway of performing consecutive coarse-graining, and the decisions rely heavily on personal judgments as well as posterior tests for any proposed CG models and simulation schemes. Hence, it is essential to have some background of the polymer species under investigation, before the underlying physics of the three CG polymer models considered in Fig. 1 may be better perceived.

Recent interest in conducting conjugated polymers arises from their solution processability, and hence, the possibility to fabricate large-area thin films at room temperature, among others. Compared with conventional synthesized polymers, however, the alternating single-/double-bond conjugation on

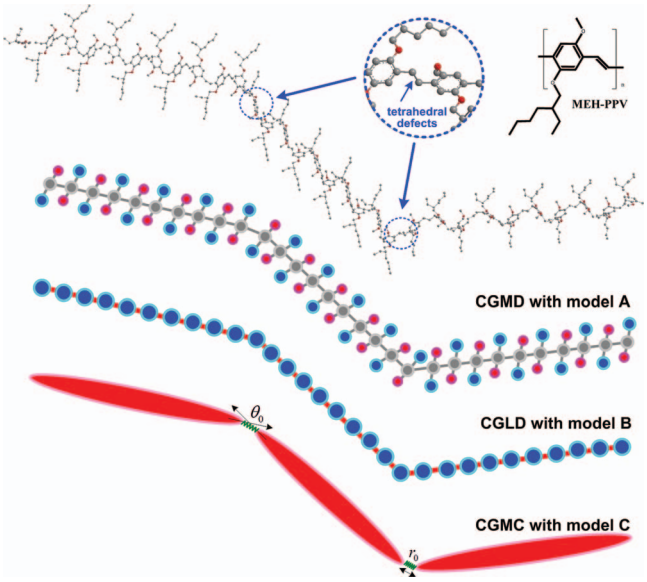

FIG. 1. Sketches illustrating (from top to bottom) AMD, CGMD, CGLD, and CGMC realizations of a single MEH-PPV (poly(2-methoxy-5-(2′-ethylhexyloxy)-1,4-phenylenevinylene)) chain in various model descriptions.

the chain backbone renders the polymer notable semiflexibility. Moreover, to promote its solubility in common organic solvents, the rigid phenyl backbone is often modified by grafting flexible alkyl/alkoxy side chains, thus imparting chemical amphiphilicity to the polymer chain as well. It turned out that there are both merits and drawbacks accompanying this amphiphilic attribute of the polymer. The appealing aspect is that a variety of solvents may be employed to fine-tune the optoelectronic properties of solution-cast thin films, at the cost that no single solvents or hybrid solvents seem to be good enough to completely suppress intra- or interchain aggregates, which, in turn, has posed stringent challenges in controlling the thin-film performance and even its reproducibility.[18–21] Thus, of fundamental and technological importance is to decipher how precise controls over the nanomorphologies of the polymer—in form of isolated chains or multichain aggregates—may be achieved through a deeper understanding of the underlying polymer–solvent interactions in the first place, as well as how favorable quenching morphologies might thus be incubated later in dried thin film. Considering the complexity in molecular attributes and a wide range of length scales involved, it can be anticipated that multiscale computing schemes should play increasingly indispensable roles in contemporary material sciences exploiting polymer semiconductors.

With the above background, it may be appreciated that the finest CG polymer model (model A) depicted in Fig. 1, which retains the distinction of the (three) major parts of a repeating unit of MEH-PPV, should allow the effects of chemical amphiphilicity in various solvent media to be unequivocally explored in usual, explicit-solvent coarse-grained molecular dynamics (CGMD) simulations. Specifically, this model treated the two asymmetric side-chain units, the backbone unit, and the solvent molecule as distinct CG particles. The construction of intra- and intermolecular force laws governing these CG particles followed standard routines utilizing the AMD simulation data of the original, atomistic model system. Nonbonding interactions between two like CG particles were modeled by a Lennard–Jones type of potential, parameterized to best mimic the radial distribution functions (RDFs) of the particle baths; a simple mixing rule was adopted to account for interactions between two unlike particle species. Several peculiar features for binary-solvent system based on this CG polymer model have previously been unveiled.[4] Of particular interest was the first revelation of coupling solvent interactions with different parts of the polymer, leading to crystal-like or layered structure of the solvent molecules in the proximity to the polymer chain. As usual, however, the corresponding CGMD simulation is very expensive, and hence, only single chains of moderate chain lengths may be investigated.

To substantially relieve the computational burden, two different strategies as have been mentioned earlier may be enforced concurrently. First, the polymer model can be further coarse-grained by lumping the whole monomer unit, including both side- and main-chain units, into a single CG particle; see model B in Fig. 1. The second involves the use of an implicit-solvent Langevin dynamics scheme that has proved to be a major breakthrough. The resulting coarse-grained Langevin dynamics (CGLD) scheme can be utilized to investigate large-scale single-chain and aggregation properties that are beyond the current reach of ordinary AMD or CGMD simulations. The reader is referred to an early article that offered a systematic comparison between CGMD and CGLD schemes.[6] Aside from the self-consistently constructed fluctuation-dissipation forces acting on the polymer molecule that mimic the essential mean-field polymer–solvent interactions, the general feature is basically no different from the CGMD model described above. Note that for a typical monomer unit that is not sufficiently large to be treated as Brownian particles, and whose dynamics show notable deviation from the predictions of the Einstein–Stokes relation, the success of this CGLD scheme in capturing both dynamic and structural properties in specific solvent media is not all that surprising, as one recalls that the equations of motion for small particles may also conform to the renowned diffusion equation on time scales substantially greater than the autocorrelation time of the particle velocities—a usually small time scale as compared with those underlying the material properties of general interest in a CG simulation.

As further coarse-grained models were pursued, we had earlier evaluated the possibility of constructing predictive CG models within conventional bead-spring picture, such as the freely rotating chain, which allows several monomer units to be treated as an effective CG bead or segment. At this enlarged CG level, only bond stretching and bending potentials need to be parameterized along with the interbead potential, which presumably determines the solvent quality.[22] The conclusion was, however, that the model fails to be fully predictive, inasmuch as the (spherical) bead diameter remains ambiguous with progressively increasing degree of coarse-graining for a semiflexible polymer like MEH-PPV that possesses ellipsoid-like segments. Without precluding the feasibility of this classical category of CG polymer models,

which indeed have their own merits, we consider below an alternative model description which is appealing in that all essential parameters for specific MEH-PPV solutions may be determined *a priori* without suffering similar constraints as noted above for bead-spring models.

B. The ellipsoid-chain model and Monte Carlo scheme

In conventional Brownian dynamics or Monte Carlo schemes for solution or melt systems, the polymer is usually coarse-grained to a considerably higher degree within the bead-spring chain picture, where a number of Kuhn segments are embedded in a CG bead or segment to warrant simple spring potentials as the relevant intramolecular potential.[23,24] For the case with semiflexible polymers, it should be obvious that spherical beads as employed in these classical models cease to be a faithful description of the model segments, especially from the perspective of excluded-volume effects. On the other hand, the so-called "pearl-necklace" model has long been serving as a potential alternative to bead-spring chains, yet it has so far found limited applications, as we remarked earlier with existing ellipsoid models. For the first time, we show how an ellipsoid-chain model—model C in Fig. 1—may be utilized as a framework to construct predictive CG polymer model for a given conjugated polymer suspended in various solvent media, as detailed below.

The basic idea can be dated back to an early effort to parameterize a large MEH-PPV oligomer (with 10 repeating unit) within the classical GB potential.[25] Because of the difficulty to solve the force expressions of a GB type of potential (see, for example, Ref. 26), however, its applications for polymer system remain rare to date. Moreover, compared with the case of small anisotropic molecules, such as liquid crystals, it has recently been elucidated that parameterization of a polymer segment with a large aspect ratio (ca. 10) within the GB potential requires a variant umbrella-sampling scheme to tackle segmental flexibility while constructing the PMFs.[27] Briefly, in sampling atomistic configurations for a pair of ellipsoidal molecules in AMD simulation, not only must the center-of-mass separation be manually controlled but two additional bond angles plus one planar angle were controlled, too, in order to cope with chain flexibility associated with a large oligomer species. After the PMFs for four representative mutual alignments (i.e., side-by-side, cross, T-shape, and end-to-end) were thus established, a general form of the GB potential can be automatically parameterized using simplex optimization, simultaneously for all four arrangements along with separation distances in the range of 0–20 Å (with a resolution of 0.1 Å). In this way, the parameterized GB potential has been shown to excellently reproduce the PMFs of not only the four ellipsoid arrangements utilized in the parameterization, but also several intermediate ones falling between the side-by-side and cross arrangements that are deemed crucial to describe the microstructure in a dense or condensed phase. Indeed, subsequent comparisons between the AMD simulation of the atomistic oligomer model and the Monte Carlo simulation of the ellipsoid CG model exhibited excellent agreement in the predicted microstructures of a dense system at two different system temperatures—indicative of excellent thermodynamic transferability.

Given the excellent performance noted above for large oligomer species, we proceed with two further refinements that are essential to construct an *ellipsoid-chain* model aimed to predict large-scale material properties of the companion polymer species dissolved in various solvent media. First, considering the role of synthesized (tetrahedral) defects, as depicted in Fig. 1, the defect locations were naturally utilized as the pivotal centers connecting adjacent ellipsoids, and the intramolecular forces associated with the connector were mimicked by a spring with both stretching and bending potentials (see Table I), and the parameter values of which were fitted from AMD simulation data describing the statistical trajectories of two connected ellipsoid molecules. The last procedure is basically no different from the usual one as adopted in constructing the new potentials governing two connected CG particles. This strategy for treating synthesized defects also facilitates a systematic investigation into their impact on fundamental chain structures, as we discuss later.

On the other hand, it is of interest to know how the PMFs constructed earlier for vacuum environment may be extended to ones for specific solvent conditions. Thus, a similar umbrella-sampling scheme was adopted, except that the pair of ellipsoids involved, each later serving as a basic CG segment in the ellipsoid-chain model, was suspended in the solvent media of interest while constructing the PMFs. Sketches showing three different cases are provided in Fig. 2. For the sake of clarity, the solvent molecules in Figs. 2(b) and 2(c) are not shown explicitly. Specifically, while Fig. 2(a) corresponds to the snapshot in vacuum environment, Figs. 2(b) and 2(c) are for those in toluene and chloroform media, respectively; see detailed specifications in the figure caption. From these illustrating examples, it can be seen that solvent has a significant impact on the detailed configurations of the MEH-PPV segments, which, in turn, brings in distinct PMFs

TABLE I. Intramolecular CG potentials and parameters used for defect locations for the ellipsoid-chain model. The results for the other two CG models were different from what given here due to a different coarse-graining level, and some information may be found in Ref. 4.

Potential functions		Notation	Parameters	
Stretching	$U_s = \frac{1}{2}k_s(r_{ij}-r_0)^2$	k_s : force constant for stretching	$k_s = 0.25\ k_B T\ \text{Å}^{-2}$	
		r_0 : equilibrium length for stretching	$r_0 = 5.6$ Å	
Bending	$U_b = \frac{1}{2}k_b(\theta_{jik}-\theta_0)^2$	k_b : force constant for bending	w/defect:	$k_b = 0.25\ k_B T\ \text{rad}^{-2}$
				$\theta_0 = 1.57$ rad
		θ_0 : equilibrium angle for bending	w/o defect:	$k_b = 33.30\ k_B T\ \text{rad}^{-2}$
				$\theta_0 = 2.88$ rad

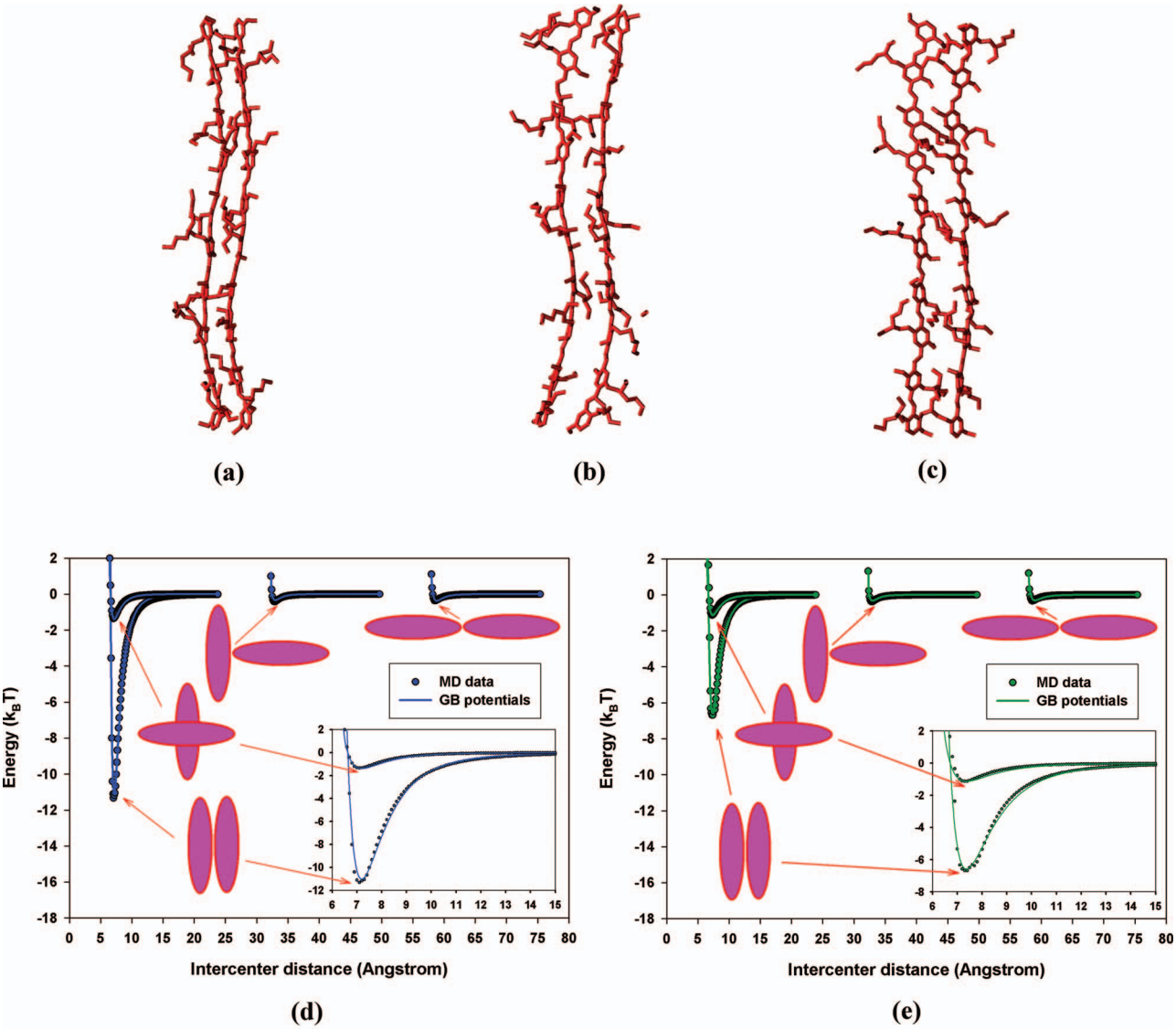

FIG. 2. Pictorial representations of a pair of 10-mer MEH-PPV in (a) vacuum, (b) toluene bath, and (c) chloroform bath (note that the solvent molecules in cases (b) and (c) were not plotted for clarity), where the PMFs have been computed using AMD simulations (symbols). Also, a comparison is shown with the predictions of the parameterized GB potential (lines) for (d) toluene or (e) chloroform medium. For each of the pair arrangements, the mean separation distance varies in the range of 0–20 Å with a uniform increment of 0.1 Å. At a given distance, AMD simulations (with DREIDING force fields) were performed using Nosé–Hoover thermostat at $T = 298$ K (with a coupling constant of 0.1 ps) for 1 ns, with an integration time step of 1 fs and a cutoff distance of 15 Å for all nonbonding interactions. This amounts to a total of 1000 nearly independent atomistic configurations later used to compute the PMFs at a given oligomer separation. The density of the solution was estimated using Nosé–Hoover *NPT* ensemble (1 atm and 298 K) to be 0.9 and 1.4 g/cm^3 for toluene and chloroform, respectively, with the total numbers of solvent particles being 5800 and 7500, respectively.

as shown in Figs. 2(d) and 2(e), for the two solvent media considered. Specifically, as an aliphatic solvent, chloroform is attractive to the side chains of MEH-PPV while being avoided by the phenyl backbone, yielding a much twisted chain backbone and overall randomized chain conformation; see Fig. 2(c). In contrast, the aromatic solvent, toluene, has a superior affinity to the MEH-PPV backbone, whose side chains contract as a result to reduce exposure to the solvent; consequently, the two chain segments remain more or less correlated upon approaching each other, similar to what has been seen in the vacuum environment (cf. Figs. 2(a) and 2(b)). Recent light-scattering experiments have revealed that for a similar hair-rod polymer, whereas toluene helps produce crystal-like structure within the polymer aggregates, no similar feature has been observed in the chloroform medium.[28] This distinguishing feature might be ascribed to the molecular contrasts as uncovered in Figs. 2(b) and 2(c), suggesting that correlated backbone alignments in conjunction with collapsed side chains might be essential for the development of ordered, crystalline structure within small aggregate species or in the bulk quenching state.

Overall, the physical pictures delineated above shed light on the way solvent medium may interfere with segmental interactions in solution, especially for an amphiphilic, semiflexible polymer like the case with typical conjugated polymers. Subsequent determinations of the parameter values within the GB potential for (extremely dilute) solution systems followed similar routes as have been outlined above and detailed

TABLE II. Parameter values for the intermolecular GB potential determined for three solvent media, each ellipsoid segment representing ten monomer units of MEH-PPV. The GB potential utilized is given by $U(\mathbf{u}_i, \mathbf{u}_j, \mathbf{r}_{ij}) = 4\varepsilon(\mathbf{u}_i, \mathbf{u}_j, \mathbf{r}_{ij})[(\xi\sigma_0/(|\mathbf{r}_{ij}| - \sigma(\mathbf{u}_i, \mathbf{u}_j, \mathbf{r}_{ij}) + \xi\sigma_0))^{12} - (\xi\sigma_0/(|\mathbf{r}_{ij}| - \sigma(\mathbf{u}_i, \mathbf{u}_j, \mathbf{r}_{ij}) + \xi\sigma_0))^6]$, where $\mathbf{u}_i$ and $\mathbf{u}_j$ are the unit vectors describing the orientations of the ellipsoid pairs i and j under consideration, $\mathbf{r}_{ij}$ is a vector connecting their geometric centers, σ_0 is related to the ellipsoidal dimension, and ξ is a dimensionless parameter which helps control the width of the potential well independent of its depth or location of the potential minimum. The parameters χ and $(\varepsilon_0, \chi', \nu, \mu)$ appear in the functionals of $\sigma(\mathbf{u}_i, \mathbf{u}_j, \mathbf{r}_{ij})$ and $\varepsilon(\mathbf{u}_i, \mathbf{u}_j, \mathbf{r}_{ij})$, respectively; see detailed specifications in Ref. 27.

Solvent	χ	χ'	ε_0 (k_BT)	σ_0 (Å)	ξ	ν	μ
Toluene	0.974	0.935	0.582	6.63	0.694	2	1
Chloroform	0.974	0.910	0.336	6.71	0.793	2	1
1:1 Hybrid	0.974	0.925	0.484	6.66	0.734	2	1

elsewhere,[27] and the results for three different solvent media are gathered in Table II. Later, a coarse-grained Monte Carlo (CGMC) scheme was employed to obtain all the results reported for the ellipsoid-chain model. It has been known, however, that Monte Carlo simulations involving large molecular segments could easily fall into traps, or the so-called "bottlenecks," in local potential field. For dilute solution, this should pose little problem, and strategies for tackling more general situations will be remarked in a later discussion section. Although there remains the possibility of utilizing a string of spherical beads to mimic a semiflexible segment, which may be simulated using usual molecular dynamics schemes (see, for example, Ref. 29), the basic feature should differ little from the model A or B considered in Fig. 1.

III. RESULTS AND DISCUSSION

The performance of the ellipsoid-chain model proposed in the preceding section for two specific single-solvent systems of MEH-PPV may be evaluated by examining the RDF for isolated chains, or by essential scaling laws reminiscent of the solvent quality. Lacking classical theory predictions on these quantities for MEH-PPV solutions, the simulation results are compared with those for two existing finer-grained models, as introduced earlier. By doing so, the efficacy (or accuracy) and efficiency of the simulations of individual CG models, denoted, respectively, as CGMD, CGLD, and CGMC, may be explored systematically. Aside from two representative single-solvent media (i.e., chloroform or toluene), a hybrid binary-solvent system with chloroform/toluene = 1:1 in number density is also examined. This particular hybrid solvent system was chosen because it provides a stringent test of the two mean-field, implicit-solvent schemes (i.e., CGLD and CGMC), as we discuss in some detail later. Afterward, the effects of synthesized defect will be scrutinized within the ellipsoid-chain model.

A. Single-chain structures in various solvent media

Figure 3 compares the (intrachain) RDF—which yields the so-called structure factor in scattering experiments—for an MEH-PPV consisting of 300 monomer units, which is close to the chain length of a commercial sample commonly used in experiment. Note that despite the capability of simulating much longer chains within the CGMC simulation—say, 3000 monomers per chain—the comparisons made here should suffice the present purpose. Due to the difference in the coarse-graining level for the three CG models considered, the RDF counts only the center-of-mass distribution of every consecutive ten monomer units, which, for example, would correspond to the distribution of the mass center of each ellipsoid within the ellipsoid-chain model. On this mapping scale, the RDF should primarily be reflective of the effects of solvent quality on the full-chain structure, because the equivalence of a 10% of tetrahedral defects in this case renders the chain sufficient flexibility. The following are some details of the simulations: The explicit-solvent CGMD simulation utilized the *NPT* ensemble at $T = 298$ K and $P = 1$ atm; details can be found in an early work.[4] For the CGLD and CGMC

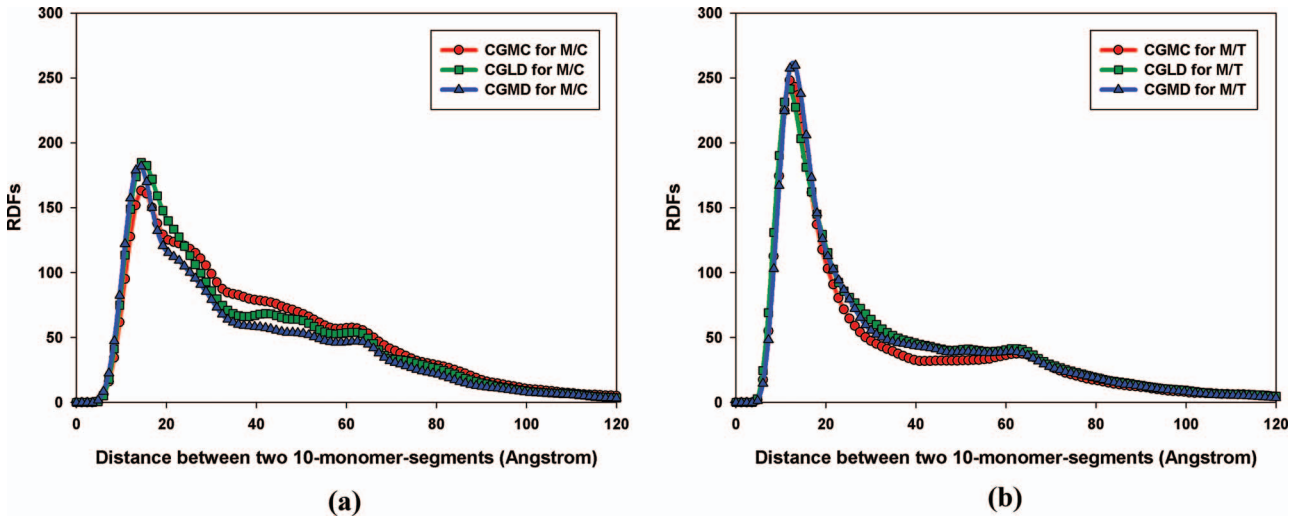

FIG. 3. Comparison of the intrachain RDFs (unnormalized) for two single-solvent media, where M/C and M/T denote the MEH-PPV/chloroform and MEH-PPV/toluene, respectively. The CGMD and CGLD simulations were both executed for a rescaled (AMD) time about 10 ns, with a time step 2 fs for CGMD and 5 fs for CGLD. The CGMC simulation involves totally 300 000 steps.[31]

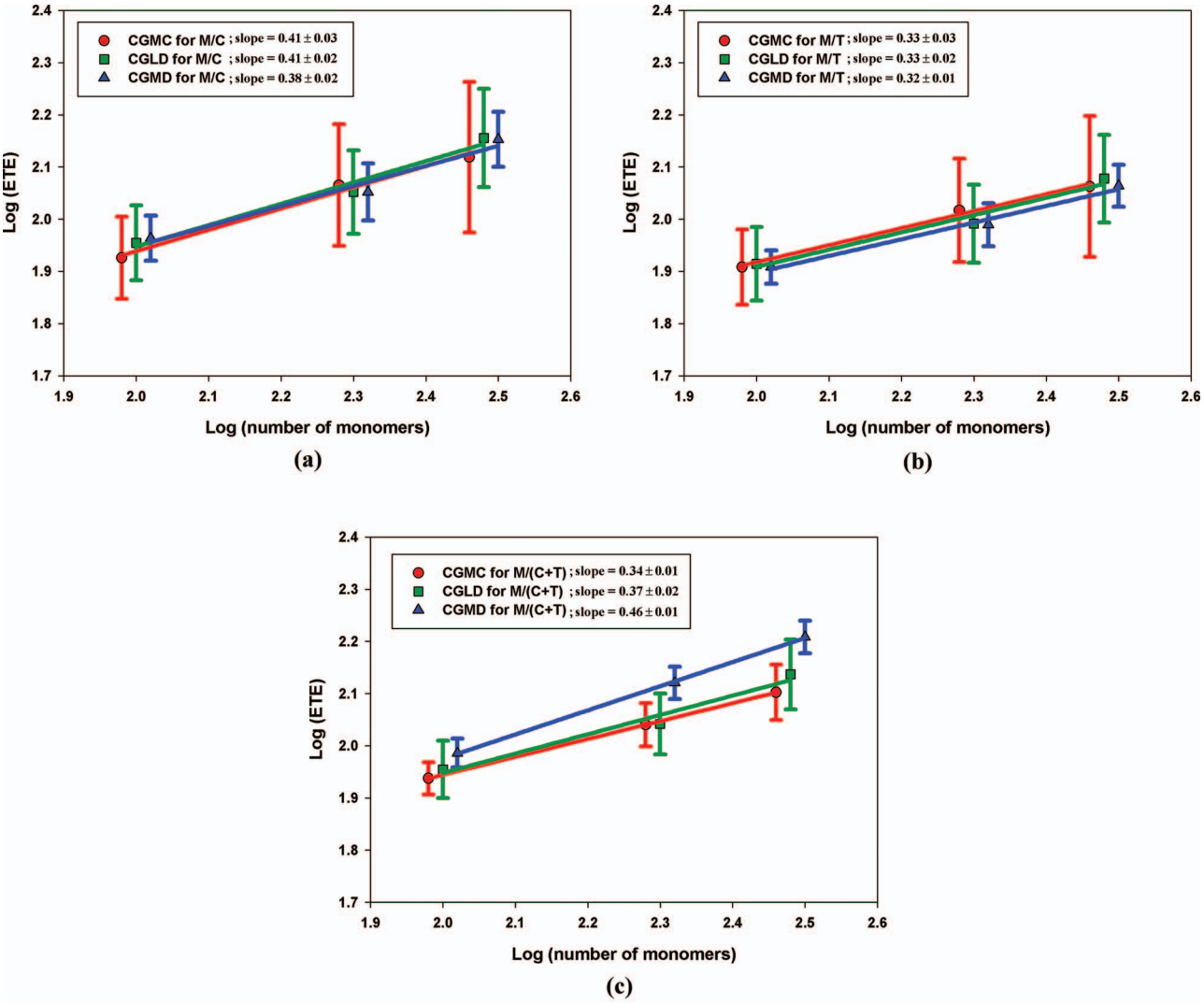

FIG. 4. The predicted scaling laws for mean end-to-end distance (ETE) of MEH-PPV in (a) chloroform, (b) toluene, and (c) chloroform/toluene = 1:1 in number density. In all cases, an ensemble average based on 100 independent chains was utilized to create the plot, and the symbols represent CGMD (triangles), CGLD (squares), and CGMC (circles). For clarity, the curves have been shifted in the *x*-axis direction by varying degree. The error bar given for the slope of each curve, which yields the solvent quality exponent, was evaluated using the mean values of ETE for the three chain lengths investigated. In this way, it is evident that only the result shown in (c) for the CGMD simulation exhibited appreciable deviation from the other two cases.

simulations, an *NVT* ensemble at the same system temperature was employed as no explicit solvents were retained. The implementation of the CGLD simulation has been documented elsewhere,[6] and the CGMC simulation of the ellipsoid-chain model basically follows the same algorithm as had been described earlier in simulating a dense ellipsoid system.[27] A major difference is in that the movement of each ellipsoid must be subject to the additional potentials involving chain connectivity for the full chain (which consists of 30 ellipsoids), and the maximum trial movements for the translation and rotation motions were automatically adjusted according to the detected total energy fluctuation;[30] see also information in Fig. 3.

It can be seen that the three CG models display fairly good agreement for the two solvent media investigated, considering the great disparity in the CG levels and attendant simulation schemes. Specifically, the simulation is able to capture the major distinction between a better (chloroform) and poorer (toluene) solvent in forging elementary single-chain structures. The polymer coil is, as expected, more compact in toluene than in chloroform, as the peak position and height would clearly indicate. The agreement has a significant implication with regard to the future prospect of utilizing a much enlarged CG level along with implicit-solvent scheme to capture the effects of different solvent media, where the solvent quality falls substantially below the theta condition, and hence, supramolecular aggregates prevail that, in general, pose notable difficulty to be directly investigated within conventional AMD or CGMD schemes.

To assess the solvent quality, Fig. 4 shows the predicted mean end-to-end distances for three different chain lengths: 100, 200, and 300 monomers, respectively. The resultant scaling law of the coil size—the mean end-to-end distance in this case—provides information about the exact solvent quality of MEH-PPV in the individual solvent system. Earlier, both single-solvent systems of MEH-PPV had been revealed to fall in the poor-solvent regime, and comparatively chloroform serves as a better solvent than toluene.[6] In Figs. 4(a)

and 4(b), it can be seen that this characteristic feature is well captured by all three CG models. On the other hand, it is intriguing to notice in Fig. 4(c) for the binary-solvent medium a pronounced discrepancy between the CGMD simulation, which utilized explicit solvents, and the two implicit-solvent schemes, i.e., CGLD and CGMC. Considering this particular solvent composition (i.e., chloroform/toluene = 1:1 in number density) was, in fact, motivated by an early finding that the CGMD simulation displayed, among all other compositions investigated, the most prominent deviations from what might be expected using simple mixing rule of the results for the two single-solvent systems.[4] In that case, there seemed to be a prominent coupling between the two solvent species when interacting with different parts of the polymer chain. From the predicted solvent quality exponents as shown in Fig. 4(c), it is interesting to note that the solvent quality (ca. 0.46) as predicted by the more reliable CGMD simulation is already close to the theta condition—which bears a theoretical exponent of 0.5, in stark contrast with the typical cases with MEH-PPV solutions, where the solvent quality was often noted to fall in considerably poor regime (i.e., below 0.4; see, for example, Figs. 4(a) and 4(b)).

Given the overall good agreement for single-solvent systems of MEH-PPV, we proceed with a comparison revealing the computing times required to obtain the results, as shown in Fig. 3, for a 300-mer MEH-PPV. From the information provided in Table III, it can be seen that the enhancement in computational efficiency is enormous when either of the two implicit-solvent schemes was utilized. Roughly, the CGMC simulation of the ellipsoid-chain model is about 300 times more efficient than the CGMD simulation of the finest CG polymer model considered, and about four times faster than the CGLD simulation which exploits a polymer model of intermediate CG level. As had been noted elsewhere for the CGMD and CGLD simulations, for instance, the difference in computing time arises mainly from the coarse-graining of the solvent molecules but not that of the polymer. In general, we expect the disparities in computational efficiency to be even dramatic when longer chains or multichain aggregates are to be simulated.

To this end, the physics underlying the success as well as the failure of the two implicit-solvent CG schemes are of interest to pursue. In the CGLD scheme, the solvent quality is, somewhat unusually, accounted for through fluctuation–dissipation forces dictating the polymer CG particles in the solvent medium. Such forces mimicked the essential polymer–solvent interactions and were directly superposed to the intermolecular forces governing polymer–polymer interactions. In this fashion, the CGLD scheme represents a special generalization of the pairwise-additive assumption commonly employed in particle dynamics simulations. In contrast, the other implicit-solvent scheme, i.e., CGMC, exploits the solvent-mediated pair interactions for suspended CG (ellipsoid) segments, the interaction forces being literally energetic and conservative in nature. Thus, the good agreement found between these two mean-field CG schemes for two representative single-solvent media seems to evoke a rethinking about the distinction that has long been imposed between conservative intermolecular forces and dissipative hydrodynamic forces in the context of coarse-grained simulations of polymer solution. In essence, the ideas of particle diffusion and associated fluctuation–dissipation forces have rested upon a timescale separation for the dynamics of the primary particle species—usually the polymer units—and the surrounding "medium" (often, the fast and uninterested solvents) that legitimates a separate treatment in tackling polymer–polymer and polymer–solvent interactions. As the polymer CG particles progressively reduce their size in more elaborate CG simulations, however, the distinction smears notwithstanding that the concept of diffusion remains applicable for small, strictly non-Brownian particles. Thus, the close agreement between the two mean-field simulations as well as their capability to well capture the explicit-solvent CGMD results appears to foresee a gradually diminishing boundary that would discriminate between entropic (e.g., CGLD) and energetic (e.g., CGMD and CGMC) formulations of solvent quality.

TABLE III. Comparison of computing times for three CG models (based on a single CPU for an 300-mer MEH-PPV).

Methods	Computing time for 1000 steps	Minimum steps to reach equilibrium	Total computing time to reach equilibrium
CGMD	530 s	1 000 000	147 h
CGLD	24 s	300 000	2 h
CGMC	29 s	70 000	34 min

This seems not to be the case, though, for the peculiar binary-solvent system investigated, and the central implication is twofold. First, the poor performance found for the CGLD scheme may be blamed for its inability to capture the coupling effects for two distinct solvents when interacting rather differently with the main- and side-chain units, respectively, of the polymer. More specifically, the failure stemmed from a nonhomogeneous distribution of solvent particles in the vicinity of the polymer chain—a highly localized feature that is not meant to be captured by any mean-field theories or schemes.

On the other hand, it might be somewhat surprising that the CGMC scheme fails in a similar manner, considering that such coupling effects should be, at least in part, embedded in the solvent-induced configurations of the two model ellipsoids used to construct the PMFs. A possible reason for this perplexing discrepancy is that the ellipsoids remain too small to foster any notable coupling when interacting with local solvent molecules. Besides, such coupling is usually reminiscent of important many-body interactions that cannot be readily captured by any mean-field theories or simulations that take advantage of effective two-body interactions.

There is, in fact, another possibility that cannot be totally precluded. Local solvent populations fluctuate rapidly over the time window within which the PMFs were evaluated, and it might well be that mainly the time-averaging feature has been captured. Such concern is motivated in part by an early observation that polymer–solvent interactions as reflected in the associated RDFs cannot be fully explained by the nominal strength of van der Waals interaction between the two species, and hence "entropic forces" of the solvents must

play an important role too.[4] It may be pondered that, when coupled with distinct (localized) energetic interactions with an amphiphilic polymer, solvent entropy could bring about conspicuous concentration fluctuations—both spatial and temporal—which help shape the effective polymer–polymer interactions in a complex solution system. A better understanding as well as a faithful account of this salient feature of polymer–solvent interactions remains open to future studies.

B. Effects of synthesized defect

Synthesized defects[32,33] have concerned scientists in the area of conjugated polymers in that they may considerably impact the performance of solution-cast thin films through a possible alteration in elementary chain structures in solution which, in turn, regulate the quenched-chain morphology. To address this rudimental issue, the CGMC simulation based on the ellipsoid-chain model has been conducted, assuming various extents of defect. Considering the usual ratio as reported in experiment,[34] three cases have been examined—0%, 5%, and 10%, respectively, for the content of tetrahedral defects. For simplicity, only uniform defect distribution was considered. Although it is possible to have, in practice, a somewhat random distribution of defects on the polymer backbone, accounting for this particular effect within the present CGMC simulation would demand availability of the PMFs for unlike ellipsoid segments, which is beyond the scope of this study. Readers who are interested in this issue may consult, for example, Ref. 32, in which the density and distribution of a different type of defect—the *cis*-defect—had been scrutinized for PPV chains for their impact on fundamental chain structure. For the first case, which is essentially defect-free, it had been postulated that the rigidity of a conjugated polymer would ultimately result in torus or ring conformations with increased chain length.[35] On the other hand, the presence of even a trace amount of defect could interrupt such tendencies and, instead, helps form more regular chain conformations as dictated by the solvent quality.

Figure 5 shows representative snapshots for the three cases considered in two different single-solvent media. Distinctive conformations can readily be seen between the chains with or without defect. For defect-free chains, an interesting feature is that the poorer solvent, toluene, may defy intrinsic chain rigidity to create various kinds of chain folding, as exemplified by Fig. 5(c). A similar situation rarely happens, however, in the better solvent, chloroform (cf. Figs. 5(c) and 5(f)). These distinguishing features, in fact, are difficult to foresee without a detailed computer simulation. Moreover, the mean coil size is much larger than the cases with defect, which we discuss next.

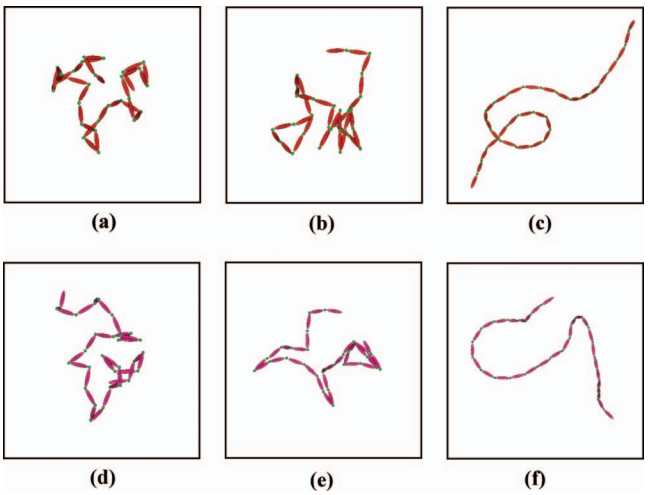

FIG. 5. Snapshots of single-chain (300-mer MEH-PPV) conformation with various amounts of defect: (a) 10%, (b) 5%, or (c) 0% in toluene; (d) 10%, (e) 5%, or (f) 0% in chloroform. The CGMC simulations were performed using *NVT* (298 K) ensemble for 300 000 steps. Understanding the real impact of defects requires a more detailed analysis; see discussion in the main text and results gathered in Table IV.

For polymer chains with various amounts of defect, revealing the disparities in fundamental chain structure requires more detailed analysis. Table IV compares the mean coil size and average segmental alignment for the six cases examined. It is found that for the two defect contents considered, i.e., 5% or 10%, the mean coil size seems little affected by the actual amount of defect, despite the fact that their size reduces substantially as compared with defect-free chains. This result may be interpreted as that, inasmuch as the chain is imparted sufficient flexibility via the presence of a certain amount of defects, the solvent quality would play the dominant role dictating the statistics of a full, long chain; also consult results shown in Figs. 3 and 4. It is therefore possible that for a real conjugated polymer—which cannot be defect-free—having chain length considerably exceeding the Kuhn length, the overall chain statistics is basically governed by the solvent quality and is less dependent on the actual amount of defect. Recall, however, that the mean coil size for MEH-PPV with as low as 5% defect content is only about one-fourth of that for defect-free chains.

TABLE IV. Single-chain structures predicted by CGMC simulation of the ellipsoid-chain model with varying degree of defect.

	Rg (nm)		ETE (nm)		OP[a]	
Defect (%)	M/T	M/C	M/T	M/C	M/T	M/C
10	5.1 ± 0.9	6.0 ± 0.7	11.5 ± 3.5	13.9 ± 4.4	0.25 ± 0.12	0.23 ± 0.15
5	5.9 ± 1.7	6.1 ± 1.3	12.3 ± 3.8	14.4 ± 2.9	0.52 ± 0.09	0.47 ± 0.16
0	20.7 ± 1.3	20.9 ± 1.1	49.6 ± 8.9	50.1 ± 8.3	0.72 ± 0.09	0.68 ± 0.11

[a]The order parameter was computed by the following ensemble average: $S = 3/2\langle(\mathbf{u}_i \cdot \mathbf{n})^2 - 1/3\rangle$, where $\mathbf{u}_i$ denotes the ith ellipsoidal vector on a chain and $\mathbf{n}$ is the "director" evaluated from the averaging of $\mathbf{n} = \langle \mathbf{u}_i \rangle$. The simulation utilized 100 independent chains and 300 000 steps to obtain the ensemble plus time averaging for each case. It is evident that segmental ordering within a chain can be readily controlled by defects, while the mean coil sizes display more complex trends as discussed in the main text.

In contrast, the amount of defect was found to determine the segmental order parameter within a chain. Namely, a greater amount of defect helps produce more disordered chain segments, *largely independent of the solvent quality*. Given that regular chain packing in the eventual quenching state, such as the $\pi-\pi$ stacking quintessential for electronic delocalization, may benefit from such ordering in the precursor solution, one might conclude that synthesized defects are detrimental to the formation of favorable $\pi-\pi$ stacking in thin film, aside from their well-known influences on the effective conjugation length and the associated spectroscopic features. Nevertheless, one should be cautious about the trade-off of numerous factors affecting the performance of a dried thin film. For instance, nearly defect-free chains would be very difficult to dissolve in any solvent media, and thereby, promote interchain aggregates, whose impact on the overall performance of a thin film remains not fully understood. Besides, a certain amount of tetrahedral defect is indeed essential for the quenched chain to proceed with a regular chain folding.[4] In summary, the simulation suggests that synthesized defects of a conjugated polymer may affect elementary chain structure in solution in various ways, depending on the solvent quality as well as the actual amount of defect. For the two different defect contents investigated, i.e., 5% or 10%, the full chain statistics is basically governed by the solvent quality and remains less sensible to the relative amount of defect. On the contrary, localized segmental ordering was readily controlled by defects while exhibiting little dependence on the particular solvent used. For ideally defect-free chains, however, the overall chain dimension enlarges significantly, and the solvent quality affects primarily the *chain morphologies* but not the mean coil size.

IV. DISCUSSION

It should now be evident that the ellipsoid-chain model introduced in prior sections for modeling conjugated polymer solutions, albeit very appealing in view of computational efficiency and the capability to capture single-chain structures in dilute single-solvent system, suffers several notable constraints that must be overcome or circumvented before one may actually benefit from its ability to treat large CG segments for a semiflexible polymer. The following aspects represent some typical challenges that must be addressed in light of the future applications: (1) The Monte Carlo simulation associated with it could become inefficient in a dense or condensed system, due to the commonplace problem of potential bottleneck as mentioned earlier. (2) Real synthesized conjugated polymers likely contain defects that differ both in their type and distribution. This essential molecular feature would require some taskwork in establishing PMFs for numerous pairs of ellipsoids with varying size. (3) For situation similar to what has been encountered with the hybrid-solvent medium, an implicit-solvent CG scheme is apparently unable to capture the effects of local solvent fluctuations which, in turn, may have some drastic influence on describing effective polymer–polymer interactions. A potential pathway these challenges may be resolved at one time is to take advantage of systematic forward/backward mappings within the hierarchy of CG models, as illustrated in Fig. 1. For instance, one may begin with a CGMC simulation based on the ellipsoid-chain model with a known and uniform defect distribution, like the case studied in the preceding section. Such a simulation should be very economic in locating (near) equilibrium conformations/morphologies of long single chains or multichain aggregates. Afterward, the model chains are backmapped to the as-efficient CGLD simulation, wherein a realistic defect distribution may be implemented that consequently modifies localized chain conformations. If necessary, such as the case of hybrid-solvent media, further backmapping may be enforced that returns the system to one for explicit-solvent CGMD simulation, or even the primal AMD simulation whenever anisotropic atomistic forces are expected to play an important role. The strategy advocated above should work for quenching systems as well, as recent studies seemed to imply.[4,5] Note that although similar backmapping schemes have customarily been adopted in conjunction with a CG simulation, few had covered a similarly wide range of CG levels. Overall, the perspectives outlined above should help enlighten an important spirit of multiscale simulations—a conventional wisdom to complement CG models or simulation schemes at various levels, and thus none of them needs to be perfect on its own.

V. CONCLUSIONS

We elaborated on the model construction and performance evaluation of a predictive ellipsoid-chain model that is especially versatile for investigating large-scale material properties of semiflexible polymers that are sensible to the specific solvents used, as well as to the synthesized defects that are ubiquitous in real polymer samples. The CGMC simulation based on it was shown to be very efficient in capturing elementary single-chain structures in two distinct single-solvent systems under dilute condition. The simulation also helped unravel interesting consequences of a trace amount of defect influencing bulk and localized chain structures, respectively. On the other hand, there were noteworthy failures associated with the two mean-field implicit-solvent CG models (i.e., CGMC and CGLD) for a binary-solvent medium, where conspicuous local concentration fluctuations—both spatial and temporal—seem to be at play. In future perspectives, we remarked on strategy that takes advantage of the coordination among various CG models and simulation schemes to warrant computational efficiency and accuracy so that it would be possible to directly investigate larger-scale, many-chain aggregate systems in various solvent media, and ultimately, to systematically explore the corresponding quenching morphologies that are central to contemporary applications with polymer semiconductors.

ACKNOWLEDGMENTS

The authors thank the reviewers' comments leading to a general improvement of this article. This work is supported by the National Science Council of the ROC. The resource provided by the National Center for High-Performance Computing is gratefully acknowledged.

[1]F. Müller-Plathe, ChemPhysChem **3**, 754 (2002).
[2]C. Peter and K. Kremer, Soft Matter **5**, 4357 (2009).
[3]J. T. Padding and W. J. Briels, J. Phys.: Condens. Matter **23**, 233101 (2011).
[4]C. K. Lee, C. C. Hua, and S. A. Chen, Macromolecules **44**, 320 (2011).
[5]C. K. Lee, C. C. Hua, and S. A. Chen, J. Phys. Chem. B **113**, 15937 (2009).
[6]C. K. Lee, C. C. Hua, and S. A. Chen, J. Phys. Chem. B **112**, 11479 (2008).
[7]A. Villa, C. Peter, and N. F. A. van der Vegt, Phys. Chem. Chem. Phys. **11**, 2077 (2009).
[8]A. Villa, N. F. A. van der Vegt, and C. Peter, Phys. Chem. Chem. Phys. **11**, 2068 (2009).
[9]J. W. Shen, C. Li, N. F. A. van der Vegt, and C. Peter, J. Chem. Theory Comput. **7**, 1916 (2011).
[10]A. V. Lyulin, M. S. Al-Barwani, M. P. Allen, M. R. Wilson, I. Neelov, and N. K. Allsopp, Macromolecules **31**, 4626 (1998).
[11]R. Berardi, D. Micheletti, L. Muccioli, M. Ricci, and C. Zannoni, J. Chem. Phys. **121**, 9123 (2004).
[12]O. Hahn, L. D. Site, and K. Kremer, Macromol. Theory Simul. **10**, 288 (2001).
[13]M. Murat and K. Kremer, J. Chem. Phys. **108**, 4340 (1998).
[14]W. Tschöp, K. Kremer, J. Batoulis, T. Bürger, and O. Hahn, Acta Polym. **49**, 61 (1998).
[15]R. Faller, Polymer **45**, 3869 (2004).
[16]W. G. Noid, J. W. Chu, G. S. Ayton, V. Krishna, S. Izvekov, G. A. Voth, A. Das, and H. C. Andersen, J. Chem. Phys. **128**, 244114 (2008).
[17]P. Carbone, H. A. Karimi-Varzaneh, and F. Müller-Plathe, Faraday Discuss. **144**, 25 (2010).
[18]T. Q. Nguyen, V. Doan, and B. J. Schwartz, J. Chem. Phys. **110**, 4068 (1999).
[19] Y. Shi, J. Liu, and Y. Yang, J. Appl. Phys. **87**, 4254 (2000).
[20]C. J. Collision, L. J. Rothberg, V. Treemaneekarn, and Y. Li, Macromolecules **34**, 2346 (2001).
[21]S. H. Chen, S. C. Su, Y. F. Huang, C. H. Su, G. Y. Peng, and S. A. Chen, Macromolecules **35**, 4229 (2002).
[22]S. C. Shie, C. K. Lee, C. C. Hua, and S. A. Chen, Macromol. Theory Simul. **19**, 179 (2010).
[23]R. B. Bird, C. F. Curtiss, R. C. Armstrong, and O. Hassager, *Dynamics of Polymeric Liquids Vol II. Kinetic Theory* (Wiley, New York, 1987).
[24]M. Doi and S. F. Edwards, *The Theory of Polymer Dynamics* (Oxford University Press, New York, 1986).
[25]J. G. Gay and B. J. Berne, J. Chem. Phys. **74**, 3316 (1981).
[26]M. Babadi, R. Everaers, and M. R. Ejtehadi, J. Chem. Phys. **124**, 174708 (2006).
[27]C. K. Lee, C. C. Hua, and S. A. Chen, J. Chem. Phys. **133**, 064902 (2010).
[28]G. Petekidis, D. Vlassopoulos, G. Fytas, and G. Fleischer, Macromolecules **31**, 1406 (1998).
[29]A. A. Darinskii, A. Zarembo, N. K. Balabaev, I. M. Neelov, and F. Sundholm, Phys. Chem. Chem. Phys. **5**, 2410 (2003).
[30]M. P. Allen and D. J. Tildesley, *Computer Simulations of Liquids* (Oxford University Press, Clarendon, 1990).
[31]D. P. Landau and K. Binder, *A Guide to Monte Carlo Simulations in Statistical Physics* (Cambridge University Press, New York, 2001).
[32]G. C. Claudio and E. R. Bittner, J. Chem. Phys. **115**, 9585 (2001).
[33]B. G. Sumpter, P. Kumar, A. Mehta, M. D. Barnes, W. A. Shelton, and R. J. Harrison, J. Phys. Chem. B **109**, 7671 (2005).
[34]A. R. Inigo, H. C. Chiu, W. Fann, Y. S. Huang, U. S. Jeng, C. H. Hsu, K. Y. Peng, and S. A. Chen, Synth. Met. **139**, 581 (2003).
[35]D. Hu, J. Yu, K. Wong, B. Bagchi, P. J. Rossky, and P. F. Barbara, Nature **405**, 1030 (2000).